RSC Advances

ROYAL SOCIETY OF CHEMISTRY

www.rsc.org/advances

Effect of Waste Cellulose Fibre on Charge Storage Capacity of Polypyrrole and Graphene/polypyrrole Electrodes for Supercapacitor Application

A.De.Adhikari[a], R.Oraon[a], S.K.Tiwari[a], Joong Hee Lee[b,c] and G.C.Nayak[a]*

[a] *Department of Applied Chemistry, ISM Dhanbad, Dhanbad 826 004, Jharkhand, India*

[b] *WCU Program, Department of BIN Fusiigon Technology, Chonbuk National University, Jeonju, Jeonbuk 561-756, Republic of Korea*

[c] *Department of Hydrogen and Fuel Cell Engineering, Chonbuk National University, Jeonju, Jeonbuk 561-756, Republic of Korea*

***Corresponding author. Tel.: Fax: +91-326-2296563. E-mail address: nayak.g.ac@ismdhanbad.ac.in (G.C. Nayak).**

Abstract:

This paper explores the possibility of dealing with two major challenges of the contemporary world, i.e., waste management and storage of energy. This study presents the extraction and application of cellulose (from waste paper) based composites for supercapacitor electrode with a view to mitigate the energy crisis. In-situ polymerization is used for the synthesis of benign composites comprising cellulose, polypyrrole (PPy) and graphene. It has been observed that inclusion of cellulose in PPy increases the specific capacitance by 318% with moderate energy density and appreciably high power density compared to PPy alone. Similar results are obtained for graphene/PPy/cellulose composite where a 273% increase of specific capacitance is observed with the incorporation of cellulose in graphene/PPy composite without deteriorating the cyclic stabilities of the electrode materials.

1. Introduction

Recent years have witnessed emergence of two major challenges on a global scale in the form of waste management and limited energy resources. On the one hand, accumulating waste materials are a potential threat to the environment. On the other hand, limited energy resources are gradually snowballing into a major crisis all across the world. Extensive researches are being carried out to tackle both the challenges.

Among various solid wastes, paper wastes occupy a significant part. Print media, packaging and academic sectors are the major producers of paper wastes. The papers used for printing newspapers, journals, office work, packaging and academic purposes are either thrown out or burned with a very small percentage being recycled. According to a report

submitted by Indian Agro and Recycled Paper Mill Association (IARPMA), about 14.6 million tonnes of waste papers are produced in India per year. Out of this, only 26% is recycled, which is insignificant as far as the environment is concerned. Waste papers generate air, water and soil pollution releasing hazardous and carcinogenic organo-halide, thereby disturbing and endangering the ecological balance. Cellulose, a major constituent of paper, can be extracted from waste papers and utilised for bio-composites and energy storage applications. Even though cellulose itself is a non-electroactive material, its application in the supercapacitor field has created enormous interest for further studies. Cellulose fibres create a multi-channel and mesoporous structure which is ideal for absorption and transport of water and essential ions through the outer and inner surface of the fibres and in the process, it acts as an electrolyte reservoir [1]. In case of cellulose fibres, there is a huge possibility for adapting to the physical and chemical properties according to the need [2]. Owing to its film-forming ability and fibrous nature, cellulose fibres can enhance the mechanical stability of cellulose-based composites.

Renewable energy sources have become a quintessential solution for the scientific community and their use is increasing by leaps and bounds. Extensive researches have been initiated on supercapacitors for utilisation of the environment-friendly materials in their applications. Super-capacitors or electrochemical capacitors, also known as the ultra-capacitors, are devices with highly specific capacitance and power density, moderate energy density, long cycle life, low maintenance and fast dynamics for charge propagation [3]. These electrochemical capacitors are the emerging energy storage devices filling the fissure between conventional capacitors and batteries.

The capacitance value of an electrochemical capacitor is determined by two storage principles: double layer capacitance and pseudo-capacitance [4]. Both contribute to the total capacitance value of the super-capacitor. These electrochemical capacitors usually contain highly porous electrode materials with high surface area, such as, carbon-based materials, that include carbon nanotube, activated carbon and graphene, contributing to the double-layer capacitance [4]. The specific surface area and pore size of the electrodes play a significant role in performance of the electrochemical capacitors [5]. The pseudo-capacitive materials, presently investigated, include metal oxides (e.g., RuO_2 [6], Ni $(OH)_2$ [7], SnO_2 [8], MnO_2 [9],etc.) and conducting polymers (e.g. Polyaniline [10], PPy [8], PEDOT [11], etc.). A few studies have also been carried out on composites based on wood fibres, cellulose fibres and carbon fibres which exhibit high specific capacitances [10, 12] as well.

One of the frontline options for the carbon-based materials used for electrochemical double layer capacitors (EDLCs) is graphene. This two-dimensional and transparent substance is the parent of all graphitic forms [13] and is the best choice for the super-capacitor application. Of late, graphene has been attracting much attention due its magnificent features like high electrical conductivity (2000 S cm^{-1}), high surface area (2630 $m^2 g^{-1}$), transparency, flexibility with Young's modulus of 10TPa, high electronic carrier mobility (200000$cm^2V^{-1}s^{-1}$) and stretchability [10]. Graphene, a single sheet material, has the highest specific capacitance of 550F/g accompanied by high intensive quantum capacitance of 21μF cm^{-2} [10]. This wonder material has opened up a new way to the material and electronic world. By preparing composites with conducting polymers, a wide compass of applications for memory backups in SRAMs (Static random-access memory), power electronics and in many other fields have been initiated. Feng *et. al.* reported a specific

capacitance of PPy (nanoparticle)/graphene composite to be 64 F/g measured in 6.0 M KOH at a current density of 0.5 A/g [14]. One of the major problems of nanomaterial-based electrodes is the inaccessible surfaces of the electrode, which drastically reduces the actual capability of the double-layered capacitance, thereby reducing the specific capacitance.

Yang Ru-Kang et al reported the fabrication and application of graphene nanosheet shelled cellulose fibers for energy storage application where they have used filter paper as the source of cellulose which resulted a specific capacitance of 252 F/g at a current density of 1 A/g in organic electrolyte $LiPF_6$ [15]. But the cost of filter paper can increase the cost of the final product. In addition organic electrolytes possessed many of the disadvantages including high cost, low conductivity (resulting in power loss), low dielectric constant (reducing the capacitance) as well as safety concerns due to the flammability and toxicity of the organic solvents [16]. The present study is focussed on the extraction of cellulose fibres from waste papers produced at the Indian School of Mines which can be a cost effective source of cellulose fibers and its application for supercapacitors. This work explored the possibility of utilization of waste material for energy storage. Effect of extracted cellulose nano-fibres from unwritten waste papers on specific capacitances of PPy and graphene/PPy composite was studied. Graphene-cellulose-based composites exhibit a great advantage as free standing and binder-free electrodes for supercapacitor application. Such 3D interwoven structures of graphene-cellulose-PPy nano sheets can have excellent mechanical stability, high specific capacitance and excellent cyclic stability [17]. The prepared composite exhibited high specific capacitance and capacity retention, facilitating storage of green energy materials along with waste management.

2. Experimental

2.1 Chemicals

Graphite powder was obtained from S.D Fine Chemicals Limited, Mumbai (India) (99.9% particle size and 100 micron). Pyrrole was obtained from SRL Pvt. Limited, nitric acid and potassium permanganate was procured from RFCL limited, New Delhi (India). Sulphuric acid (98% pure), ortho-phosphoric acid 88%, methanol, sodium hydroxide, acetic acid glacial 99-100% and hydrogen peroxide were obtained from Merck Specialist Pvt. Limited, Mumbai. Sodium Chlorite was obtained from Loba Chemie Pvt. Limited, Mumbai. Ammonium persulphate was procured from CDH Pvt. Limited, New Delhi (India). The waste papers used were the discarded unwritten sections of answer sheets of students from the Indian School of Mines, Dhanbad. All the chemicals were used as received without any further purification.

2.2 Synthesis of Graphene

Graphene was synthesized by improved Hummer method [18]. Briefly graphite (2g), H_3PO4: H_2SO_4 (9:1) (100 ml) were mixed and stirred in an ice bath. To this, 15 gm of $KMnO_4$ was added very slowly. This reaction mixture was stirred at room temperature for 2 hours. Subsequently, 100 ml of deionised water was added and the temperature was increased to 90^0 C for 30 minutes. To this, 100ml of water was added slowly followed by gradual addition of 30% of H_2O_2 in absence of light. The reaction mixture was filtered, washed with water until pH came to around 7. The graphene oxide, thus obtained, was dispersed in water/methanol (1:5) mixture and purified with three repeated centrifugation steps of 17,000 rpm for 10 minutes. The prepared graphene oxide was reduced by diluted NaOH to obtain graphene [19].

2.3 Extraction of Cellulose Fibres from Waste Papers

Cellulose fibres were extracted by dissolving waste papers in 5% NaOH [20]. The dissolution process was carried out in a mechanical stirrer at 4000 RPM. The entire solution was stirred at 80^0C for 3 hours to remove hemicellulose present in the pulp of waste paper. This was followed by several washings till the neutral p^H. The bleaching treatment was carried out with sodium chlorite and acetic acid in water at 80^0C till the coloured substances were removed. The remaining slight grey colour was removed with water. The purpose of this bleaching process was to remove the remaining lignin. The solution was then subjected to acid hydrolysis with 64% sulphuric acid for 1hour at 70^0C. Finally, it was neutralized with water to get crystalline cellulose fibres (C).

2.4. Preparation of Composite

2.4.1. *Preparation of Graphene/PPy Composite (GP)*

50 mg of the prepared graphene was dispersed in 50 ml of deionised water and sonicated for about 15 minutes. After complete dispersion, 1ml pyrrole was slowly added to it with constant stirring. The solution was further sonicated for 15 minutes. To the above solution, 2.5g ammonium persulphate (APS) in 50ml water was gradually added. Then it was stirred for 30 minutes with the help of magnetic stirrer and followed by 15 minutes sonication. The beaker was covered and refrigerated overnight for complete polymerization. The resulted solution was filtered, washed and dried to obtain the composite and marked as GP.

2.4.2. *Preparation of Cellulose/PPy Composite (CP)*

50 mg of extracted cellulose was sonicated for 15 minutes in 50ml of water followed by slow addition of 1ml pyrrole. The solution was further sonicated for 15 minutes. To the above solution, 2.5g APS in 50ml water was gradually added. It was then kept under magnetic stirring for 30 minutes followed by 15 minutes of sonication. The beaker was covered and refrigerated overnight for complete polymerization. The solution was filtered, washed and dried to obtain the composite CP.

2.4.3. *Preparation of Cellulose/Graphene/PPy Composite (CGP)*

Cellulose and graphene-based PPy composite was prepared by following the same process as in CP in presence of Graphene. Briefly, 50 mg of extracted cellulose was sonicated in 50 ml of water followed by addition of 50 mg of graphene. The whole solution was sonicated for 15 minutes. 1 ml of pyrrole was slowly added to this dispersion with stirring followed by slow addition of 50 ml of APS solution. The whole solution was stirred for 30 minutes and finally sonicated for 15 minutes. The beaker was covered and refrigerated overnight. The solution was then filtered, washed and dried to obtain the composite CGP.

3. Characterizations

The crystallinity of cellulose fibre and its composites were analysed by XRD (Bruker D 8 Focus). The diffraction data were recorded at a scan rate of 1^{o}/min for 2θ angles between 10^{o} and 35^{o}. The Fourier transform infrared spectroscopy (FT-IR) was carried out using Perkin Elmer Spectrum RXI and KBr pellets within a range of 4000-500 cm^{-1}. The surface morphology of the composite at lower resolution as well as higher resolution was characterized by Scanning Electron Microscope (SEM) using HITACHI S 3400N and field

emission scanning electron microscope (FESEM) using Supra 55 (Carl Zeiss, Germany), respectively.

The electrochemical properties of cellulose-based composites were characterized by three electrode system using 1 M KCl as electrolyte at room temperature in CH instrument (Model No. CHI 760D). The working electrode was prepared by pelletizing a small amount of the sample on platinum sheet and mounted on the electrochemical cell. Ag/AgCl and platinum wire was used as reference and counter electrode, respectively. The electrochemical impedance spectrum (EIS) was analysed by 5mV of amplitude and in the frequency range of 1 Hz to 100000Hz. Cyclic voltammetry was performed in the potential range of 0 to 0.8 V at scan rates of 10, 20, 50 and 100mV/sec. Specific capacitance, energy density and power density were calculated from CV using the following formulas:

Specific capacitance = $\int IdV/m\,(SR)\,V$ ----- (1) [8]

Where, I=current density; m=Mass of sample; V=potential and SR= scan rate

Energy density $=CV^2/2$ ----- (2) [21]

Where, C= Specific capacitance and V= Potential

Power density $=E/\Delta t$ ----- (3) [21]

Where, E= Energy density and Δt= time.

The charging-discharging study of the composite was carried out by galvanostatic charge and discharge in the range of 0 to 0.8 V at a current density of 1 A/g using Biologic CLB2000.

The specific capacitance was obtained from the discharge process according to the following equation:

Specific Capacitance $=I\Delta t/\Delta V*m$ -------- (4) [22]

Where, I= Current loaded, Δt= discharge time in sec, ΔV=Potential change during the discharge process, m= mass of the electrode material.

4. Results and Discussion

Crystal nature of the extracted cellulose fibre and its composites were analysed by XRD and is shown in figure 1. Two characteristic peaks of cellulose, corresponding to the crystal planes (110) and (200), were observed in XRD curve of cellulose fibre at around 2θ values of 16 and 23 degree, respectively, which confirmed that the structure of the cellulose fibre was not destroyed during the extraction process [23,9]. However, the two intense peaks of cellulose disappeared in XRD patterns of CP and CGP due to the coating of PPy on cellulose fibre. Owing to its amorphous nature, PPy does not possess a crystalline peak in its XRD pattern (figure 1). Coating of PPy on cellulose fibre shielded the cellulose fibre from X-Ray diffraction. As a result, crystalline peaks of cellulose fibre disappeared in CP and CGP and a broad peak, similar to PPy, was observed. This confirmed the successful coating of cellulose fibres with PPy.

FTIR spectra of various samples are shown in figure 2.The spectrum shows a peak at 1055 cm^{-1} for sample C, which is the representative peak of anti-symmetric bridge stretching of C-O-C groups in cellulose [24]. The band near 1375 cm^{-1} could be ascribed to $-CH_2$ vibrations in cellulose [24]. The peak at 1653 cm^{-1} could be attributed to the OH deformation

of absorbed water on cellulose fibre [25]. The peak in the range of 2370 cm^{-1} in case of C signifies the glucose ring stretching of cellulose [26].The broad band near 3366 cm^{-1} is the representative band of aromatic O-H vibration, present in CA [24], which is responsible for hydrogen bonding among the cellulose fibres. All the peaks in the spectrum of C confirmed the successful extraction of cellulose fibres from waste papers.

In case of composites CP and CGP, the bands at 919and 878 cm^{-1} indicated the out-of-plane deformation of PPy rings [27, 28]. The peak around 1544 cm^{-1} can be assigned to the five-membered ring stretching and free C–N stretching vibrations of pyrrole ring [29]. The broad aromatic O-H frequency disappeared in case of CP and CGP and a broad band at around 3300cm^{-1}-3500cm^{-1} appeared due to the N-H stretching vibration of PPy rings [22]. This suggests that hydrogen bonding is no longer prevalent between cellulose fibres due to the incorporation of graphene and coating of PPy. The disappearance of the peak proves that PPy and graphene diminish the hydrogen bonding tendency of the cellulosic chains by acting as a barrier layer. Pure PPy gave a peak at 1536 cm^{-1} due to the C-C stretching vibration in pyrrole ring, which is shifted to 1544 cm^{-1} in both CP and CGP. This shift can be due to the interaction between–N–H of pyrrole ring and the -OH group of cellulose [30, 31]. The PPy coating upon cellulose fibres and dispersion state of graphene in CP and CGP have been discussed elaborately in morphological analysis section (SEM and FESEM analysis)

The surface morphologies of C, PPy, CP, GP and CGP were analysed by SEM (at low magnification) and FESEM (at high magnification).These are depicted in figures 3 and 4, respectively. The SEM image of C shows a micro-fibrous and smooth nature while PPy has a particulate morphology (figure 4b). Polymerization of pyrrole, in presence of cellulose fibres, changed the morphology of PPy from particulate to that of fibrous. During the

polymerization, cellulosic fibres acted like templates to give PPy its fibrous morphology. This was in accordance with the XRD analysis where crystalline peaks of cellulose were missing for CP due to the coating of cellulosic fibres with PPy. The SEM image of GP shows a sheet-like morphology due to the coating of PPy over graphene sheets as depicted in figure 3c. For the composite CGP (figure 3d), a similar sheet-like morphology was observed.

To further confirm the nanoscale morphology, all the samples were analysed by FESEM at a higher magnification. Figure 4a shows the compact and fibrous nature of cellulose fibres, which is attributed to the intramolecular H-bonding. Although at lower magnification, the cellulose fibres could be observed on the micrometre scale, the FESEM image confirmed that many nanofibers were clustered together via hydrogen bonding. However, the FESEM images of CP and CGP, depicted in figures 4c and 4e, exhibit quite different morphology due to a coating of PPy and presence of graphene. Figure 4c shows that the nanocellulose fibre clusters were broken down with PPy coating. PPy might have diminished the hydrogen bonding tendency of cellulose fibres by creating a barrier along their surface. Even though there is a possibility of hydrogen bonding between PPy chains, it is much weaker and less dense as compared to cellulose-cellulose hydrogen bonding interaction due to which the coated fibres were separated from one another. In contrast to the particle morphology of PPy (figure 4b), the GP system showed a sheet-like morphology (figure 4d). Incorporation of cellulose fibres in graphene/PPy composite created a net-like morphology (figure 4e) on the coated graphene sheets (not observed in the GP system), which could enhance the porosity of the whole system and electrolyte access during charging and discharging cycles. A schematic diagram of coating and stabilization process is given in figure 5.

Surface area of electrode material is a major factor for the electrochemical performance of supercapacitor. He et al studied microwave assisted $ZnCl_2$ activated biomass derived mesoporous carbon and reported that bigger average pore size and uniform structure along with high surface area can enhance the specific capacitance [32]. Similar study with 3 D porous hollow graphene ball derived from coal tar pitch produced a specific capacitance of 321 F/g at 0.05 A/g due to well-balanced ratio of macro, meso and microspores structure of electrode material as well as high surface area [33]. The Brunauer - Emmett - Teller (BET) analysis of our samples shows a specific surface area of 201, 342 and 508 m^2/g for C, CP and CGP, respectively (See supporting information). These values are much higher than the reported values for PPy (19.2 m^2/g) [34] and graphene PPy nanocomposites (98.6 m^2/g) [35]. The pore size of CP and CGP are also lies in the mesoporous range. This suggests that cellulose plays a significant role in enhancing the specific surface area and hence can influence the electrochemical properties of electrode materials.

To evaluate the effect of cellulose on PPy and graphene PPy composites, cyclic voltammetry experiments were carried out at scan rates of 10, 20, 50 and 100 m V/s and the outcomes are shown in figure 6. A potential window was selected from 0 to 0.8 V so as to avoid the PPy over oxidation by reversing the anodic potential scan immediately before the onset of the over oxidation peak [36]. In addition to the double-layer capacitance, manifestations of hetero-atoms and other functional groups also contributed pseudo-capacitance to the whole system [37, 38].One can understand that the shape of the CV loop should have a larger surface area with low contact resistance. However, a larger resistance contorts the loop resulting in a narrower loop with an oblique angle [2]. The cyclic voltammograms of C exhibited negligible electro activity, and, hence, did not contribute

significantly to the capacitance. The hydrogen bonding among the cellulose fibres also restricted the separation of cellulose nano-fibres from one another, limiting its double layer capacitance. But on coating of PPy on the cellulose fibres (CP), the hydrogen bonding interaction among the cellulosic chains reduced to some extent, resulting in the separation of the fibres (as discussed in SEM and FESEM). Thus, even though cellulose is non-conducting, the porosity and surface area can be expanded by incorporating PPy. Moreover, there is an added advantage on incorporating cellulose. It can act as a very good electrolyte reservoir which enhanced ions transfer as reported by Zhu *et. al.* [1]. Thus, the specific capacitance obtained in case of CP was about 51F/g, which is 318% higher as compared to pure PPy which possesses only 16F/g capacitance. Hence, the presence of cellulose fibres plays a significant role in enhancing the low capacitive value of pure PPy. Apart from providing the template surface for the PPy growth, cellulose fibres also reinforce the brittle PPy and act as a binder which increases the mechanical stability.

To further analyse the effect of cellulose fibres on specific capacitance, the Graphene/ PPy system with and without cellulose fibres was studied. It was found that CGP possessed a higher specific capacitance compared to GP. Since the amount of pyrrole and graphene for both GP and CGP were the same, the enhancement in specific capacitance could be correlated to the incorporation of cellulose fibres. In this present work, GP contributes a specific capacitance of 89 F/g. However, on incorporation of cellulosic fibres (CGP), it increases to around 243F/g, which is 273% higher. It was assumed that in case of GP, the entire surface area of Graphene/PPy nanosheets would not be accessible by the electrolyte, which would limit its double-layered capacitance. Incorporation of cellulose fibres enhanced the electrolyte accessibility and the electrical double-layer capacitance. However, further

characterizations are required to establish this mechanism. In presence of graphene sheets, the cellulose fibres were also stabilized where graphene acted as a barrier to the hydrogen bonding tendency of the cellulose fibres. These separated cellulosic fibres acted as electrolyte reservoir and enhanced the electrolyte access by the coated graphene sheets and increased its specific capacitance.

A comparative representation of specific capacitance (SC), energy density (ED) and power density (PD) of various samples are depicted in figure 7. Previously various studies have reported that MWCNT-cellulose-based super capacitors showed a specific capacitance of 145F/g in 6(M) aqueous KOH [39]. But in this case, the composites, CP and CGP, gained specific capacitances of 51 F/g and 243 F/g, respectively, in 0.1(M) KCl solution at a scan rate of 10mV. The values were, thus, much higher than the previously reported values. The ED and PD of these composites were also remarkably high, making the composites to be a quirky contestant for the super capacitor applications.

Charge-discharge capability of all the samples were analysed by galvanostatic charge and discharge and are presented in figure 8. The symmetrical and triangular characteristics of charging- discharging curves indicate excellent electrochemical capability and redox process depicting good reversibility and suggesting major contribution from EDLC [40].The discharge time of CGP was found to be the best among all the studied electrode materials, which can be correlated to its higher specific capacitance. This improvement in the electrochemical performance of the CGP composites can be ascribed to the synergistic effect of graphene and PPy-coated cellulose fibres. The superior functioning of the charging-discharging of CGP can also be supported by the very low potential drop as observed from

the charge-discharge plots. The potential drop in case of PPy can be minimised by incorporating the porous cellulose fibres as observed in CP. Similarly, discharge time of CGP was found to be higher than GP, which is in accordance with the specific capacitance calculation, where the latter possessed better specific capacitance. The cyclic stability for 2000 cycles was performed which established that incorporation of cellulose fibres does not decrease the cyclic stabilities of the electrode materials (figure 9). The plot established that there is about 94% retention of specific capacitance in case of the composite CGP, which is comparable with the GP system. Similar results were also obtained for the CP and PPy systems where cyclic stability was not hampered by the incorporation of the cellulose fibres.

To further analyse the advantages of CGP and CP over pure C, PPy and GP as supercapacitor electrode materials, the electrochemical properties of the cellulose-based composites were characterized by electrochemical impedance spectroscopy (EIS). Figure 10 shows the nyquist plots of the composite. It reveals the electrochemical impedance spectroscopy by illustrating the electron transport properties of the prepared composites. The plot corresponding to pure PPy and cellulose-based composites shows a different behaviour in high and low frequency region. The plot corresponding to the pure PPy shows a very high solution resistance as compared to the other composites. By coating this PPy on graphene as in composite GP, the solution resistance was reduced to an extent due to the addition of highly conducting graphene. The high frequency region is attributed to the combined charge transfer and double layer capacitance. The composites showed a semicircle in the high frequency region and almost a straight line in the low frequency region. The latter depicted the mass transfer related to the Warburg impedance [41]. The low frequency region of the spectra is associated with the adsorption process, microscopic charge transfer and surface

roughness [42]. Careful inspection of the plots at higher frequencies revealed that the composites, namely, CP and CGP, have higher knee frequencies than that of the pure PPy and GP and this illustrates much higher charge transfer rates [43]. The Warburg region with regard to CGP is almost straight as compared to the pure PPy and GP. This establishes that incorporation of cellulose enhances the accessibility of electrolyte by the electrode material because of the fibrous and porous nature of the cellulose.

5. Conclusion

This study has explored the effect of cellulose fibres, extracted from waste paper, on energy storage capabilities of PPy- and Graphene/PPy-based electrode materials. Cellulose fibres were extracted from and incorporated to PPy and graphene/polymer composites by in situ polymerization process. It was found that incorporation of cellulose fibre enhanced the specific capacitance, power density and energy density of the electrode materials, which is correlated to a better electrolyte access in presence of cellulose fibres where these fibres act as an electrolyte reservoir and transfer media.

Reference

1 H.Zhu, Z. Jia, Y.Chen, N. Weadock, J. Wan, O. Vaaland, X. Han, T. Li and L. Hu, *Nano Lett.* 2013, **13**, 3093-3100.

2 D. Hulicova, J. Yamashita, Y. Soneda, H. Hatori, and M. Kodama, *Chem. Mater.*2005, **17**, 1241.

3 L. L. Zhang, R. Zhou and X. S. Zhao, *J. Mater.Chem*. 2010, **20**, 5983–5992.

4 A. Davies, P. Audette, B. Farrow, F. Hassan, Z. Chen, J.Y. Choi and A. Yu, *J. Phys. Chem. C.* 2011, **115**, 17612-17620.

5 C. Agnèsa, M. Holzingera, A. Le Goffa, B. Reuillarda, K. Elouarzakia, S. Tingryb and S. Cosnier, *Energy Environ.Sci*, 2012, **00**, 1-3.

6 Z.S. Wu, D. W. Wang, W. Ren, J. Zhao, G. Zhou, F. Li and H. M. Cheng, *Adv. Funct. Mater.*2010, **20**, 3595–3602.

7 H. Jiang, T. Zhao, C. Li and J. Ma, *J. Mater. Chem*., 2011, **21**, 3818.

8 W. Wang, Q. Hao, W. Lei, X. Xia and X. Wang, *RSC Adv.,* 2012, **2**, 10268–10274.

9 S. Chen, J. Zhu, X. Wu, Q. Han and X. Wang, *ACS Nano*, 2010, **4**, 2822-2830.

10 M. Sawangphruk, M. Suksomboon, K. Kongsupornsak,J. Khuntilo, P. Srimuk,Y. Sanguansak, P.Klunbud,P. Sukthaa and P. Chiochan, *J. Mater. Chem. A*, 2013, **1**, 9630.

11 F. Alvi, M. K. Ram, P.A. Basnayaka, E. Stefanakos, Y. Goswami, A. Kumar, *Electrochim. Acta* 2011, **56**, 9406-9412.

12 Y. J. Kang, S.J. Chun,S.S. Lee, B.Y. Kim,J. H. Kim, H. Chung, S.Y.Lee and Woong Kim, *ACS Nano*, 2012, **6(7)**, 6400-6406.

13 C. N. R. Rao, A. K. Sood, K. S. Subrahmanyam, and A. Govindaraj, *Angew.chem.Int.Ed*.,2009, **48**, 7752-7777.

14 X. Feng, Z. Yan, R. Li, X. Liu and W. Hou*, Polym. Bull.*, 2013, **70**, 2291-2304.

15 Y.Kang, Y.Li, F.Hou, Y.Wen and D.Su, *Nanoscale*, 2012, **4**, 3248-3253.

16 L. L. Zhang and X. S. Zhao, Chem. Soc. Rev., 2009, 38, 2520-2531.

17 Z. Wang, Y. Su, D. W. Wang, F. Li, J. Du andH. M. Cheng, *Adv. Energy Mater*., 2011,**1**, 917-922.

18 D.C. Marcano, D. V. Kosynkin, J. M. Berlin, A. Sinitskii, Z. Sun, A. Slesarev, L.B. Alemany, W. Lu and J.M. Tour *Acs Nano* ,2010, **4**, 4806-4814.

19 X. Fan, W. Peng, Y. Li, X. Li, S. Wang, G. Zhang and F. Zhang, *Adv. Mater* ,2008,**20**, 4490-4493.

20 H. Takagi, A. N. Nakagaito, M. S. A. Bistamam, *J. Reinf. Plast. Compos*. , 2013, **32,** 1542-1546.

21 J. Yan, T. Wei, B. Shao, Z. Fan, W. Qian, M. Zhang and F. Wei, *Carbon,* 2010, **48**, 487-493.

22 C. Zhu, J. Zhai, D. Wen and S. Dong, *J. Mater. Chem*., 2012,**22**,6300-6306 .

23 Q. Zhang, M. Benoit, K.D.O. Vigier, J. Barrault, G. Jégou , M. Philippe and F. Jérôme, *Green Chem.*, 2013, **15**, 963-969.

24 M. Fan, D. Dai and B. Huang, *Fourier transform-Material Analysis,* ed. Salih Mohammed Salih, InTech, Ch. 3, pp. 45-68.

25 A.Sdrobis, G.E. Ioanide, T.Stevanovic and C. Vasile, *Polym. Int*, 2012,**61**, 1767-1777.

26 S. F.S. Draman,,R. Daik, , F.A. Latif, and S.M. E.Sheikh, *BioRes.*, 2014, **9**, 8-23.

27 H. J. Kharat, K. P. Kakde, P. A. Savale, K. Datta, P. Ghosh and M. D. Shirsat*Polym. Adv. Technol,* 2007, **18**, 397–402.

28 J. T. L. Navarrete and G. Zerbi, *J. Chem. Phys.,* 1991,**94,** 957-964.

29 J. Jang and J.H. Oh, *Chem.Commun.*2002, **19**,2200-2201.

30 D. Müller, C.R. Rambo, D.O.S.Recouvreux, L.M. Porto and G.M.O. Barra, *Synthetic Met*., 2011, **161**, 106-111.

31 J.H. Johnston, F.M. Kelly, J. Moraes, T. Borrmann, D. Flynn, *Curr. Appl. Phys*, 2006,**6**, 587-590.

32 X. He, P. Ling, J. Qui, M. Yu, X.Zhang, C.Yu and M.Zheng*, J.Power Sources,* 2013, **240**, 109-113

33 X.He, H.Zhang, H.Zhang, X.Li, N.Xiao and J.Qui, J. Mater.Chem, A, 2014, **2**, 19633.

34 M. Sharma, G. I. N. Waterhouse , S W.C. Loader , S Garg , D Svirskis International Journal of Pharmaceutics 443 (2013) 163–168.

35 L.Q. Fan, G. J. Liu, J.H. Wu, L. Liu, J.M. Lin, Y.L. Wei, Electrochimica Acta 137 (2014) 26–33.

36 Y.C. Lin, J.Cho, G.A.Tompsett, P.R. Westmoreland, G.W. Huber, *J. Phys. Chem. C* 2009, ***113***, 20097–20107.

37 G. Nystro¨m, A. Mihranyan, A. Razaq, T. Lindstro¨m, L. Nyholm, and M. Strømme, *J. Phys. Chem. B,* 2010, **114***,* 4178–4182.

38 A. Razaq, L. Nyholm,M. Sjödin, M.Strømme and A. Mihranyan, *Adv.Energy Mater*,2012, **2**, 445-454.

39 B.J. Yoon, S.H. Jeong, K.H. Lee, H.S. Kim, C.G. Park and J.H. Han,*Chem. Phys. Lett.* 2004, **388**, 170.

40 L.Deng, R.J. Young, I.A.Kinloch, A.M.Abdelkader, S. M. Holmes, D.A. H. Rio and S.J. Eichhorn, *ACS.Appl.Mater.Interface*, 2013,**5**,9983-9990.

41 H.Pang, C. Wei, X. Li, G. Li, Y.Ma, S. Li, J. Chen and J. Zhang, *Sci. Rep*, 2014**, 4**, 3577.

42 S. Hong, W. Chen, H. Q. Luo and N. B. Li, *Elsevier* , 2012, **57,** 270-278.

43 P.A. Basnayaka, M. K. Ram, L. Stefanakos and A. Kumar, *Graphene*, 2013, **2**, 81-87.

Figures

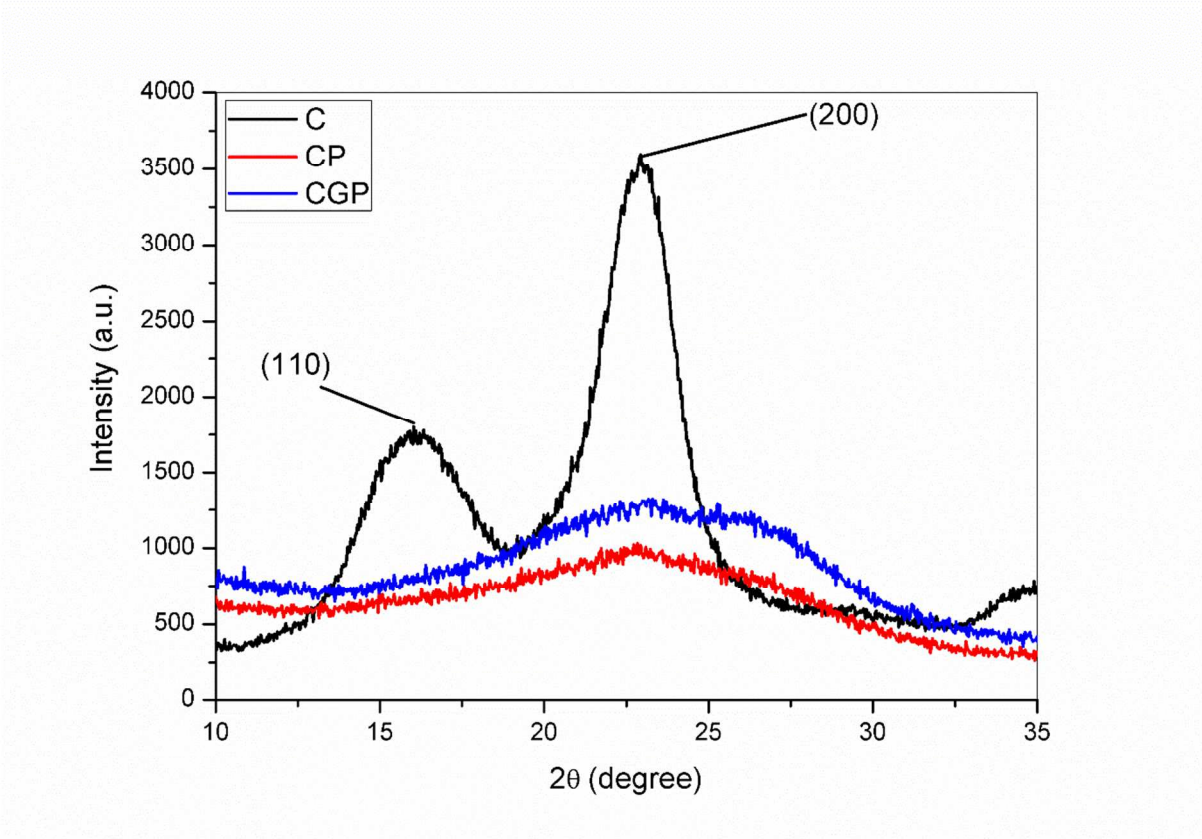

Figure 1: XRD Plot of C, CP and CGP

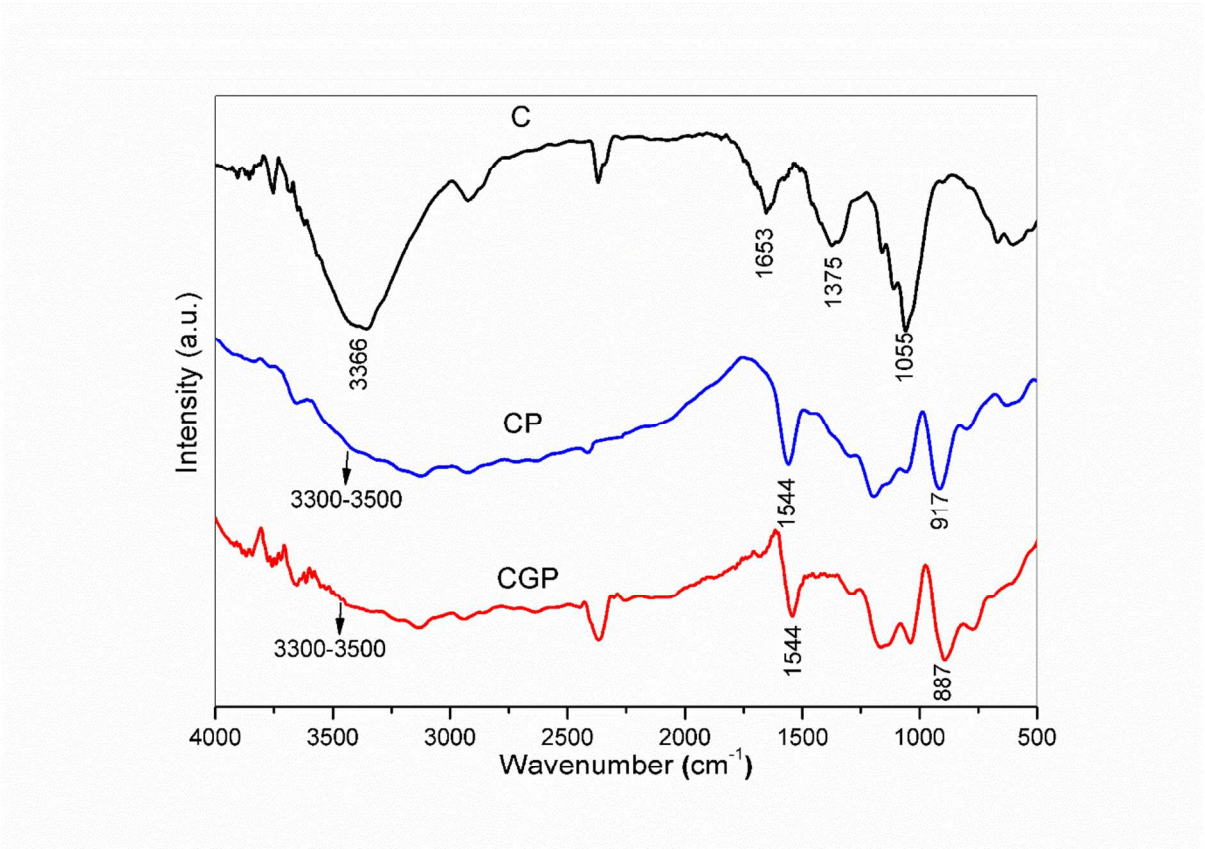

Figure 2: FTIR Spectra of C, CP and CGP

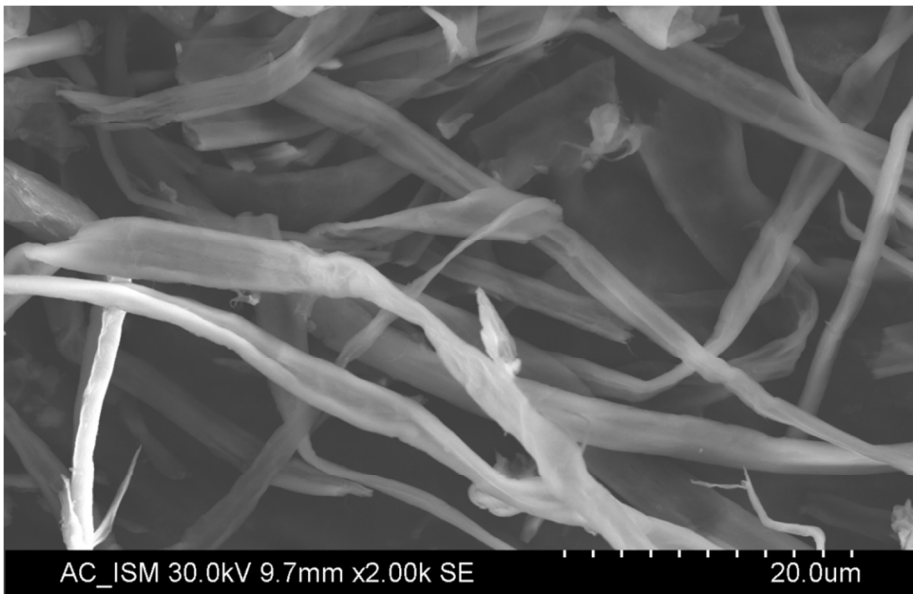

Figure 3a: SEM Image of C

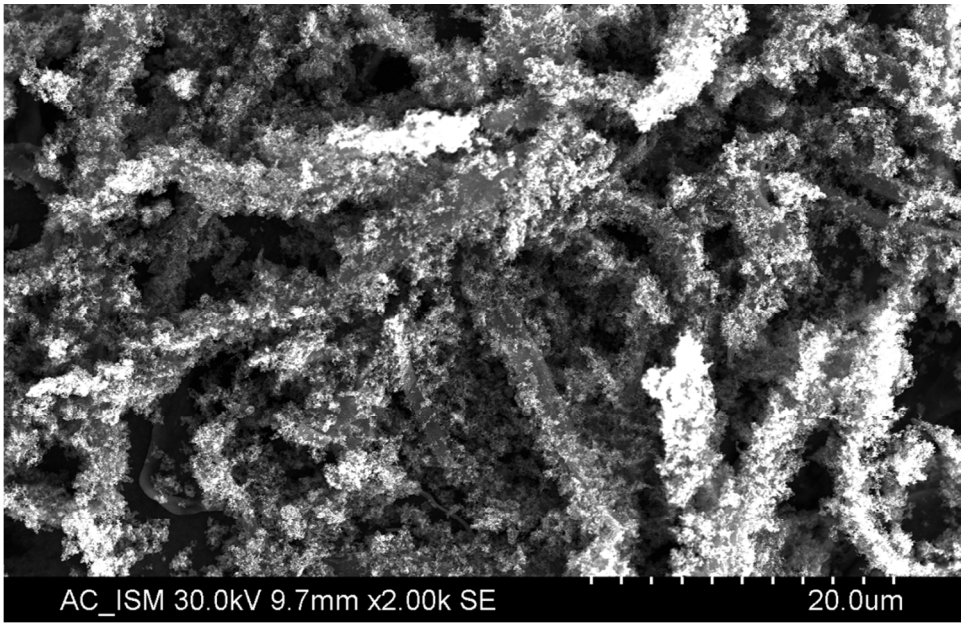

Figure 3 (b): SEM Image of CP

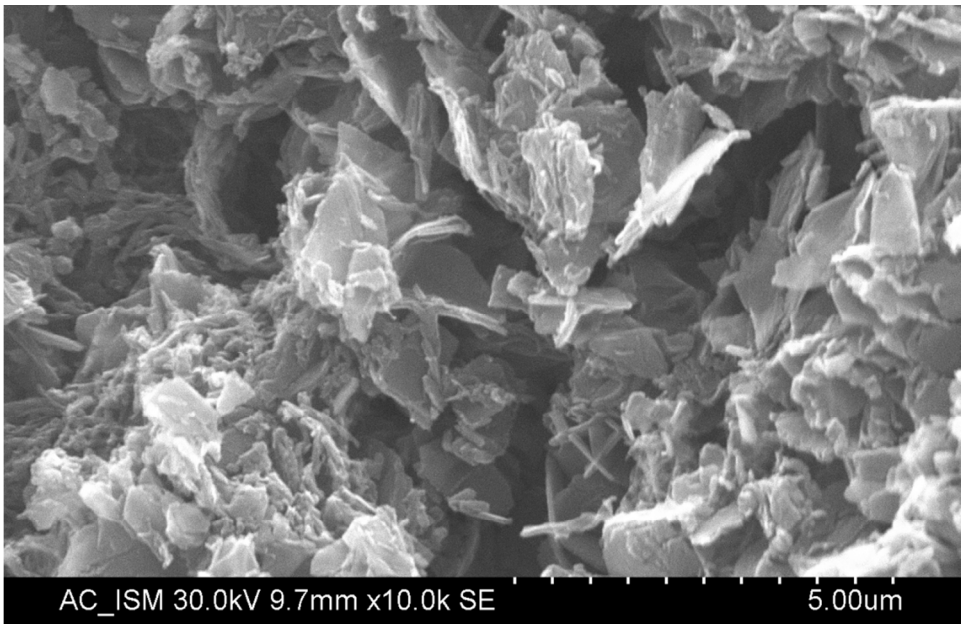

Figure 3c: SEM Image of GP

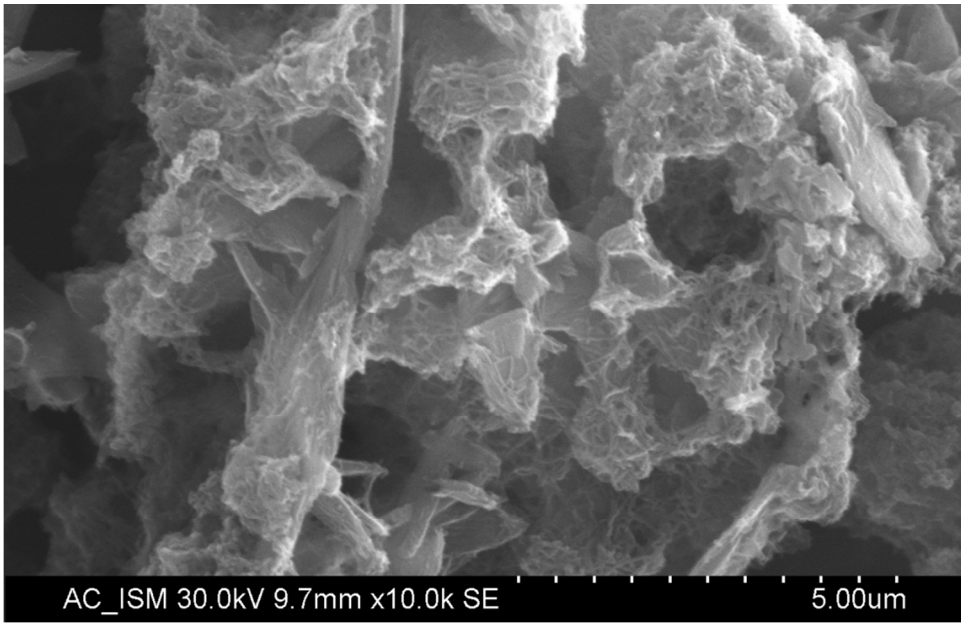

Figure 3d: SEM Image of CGP

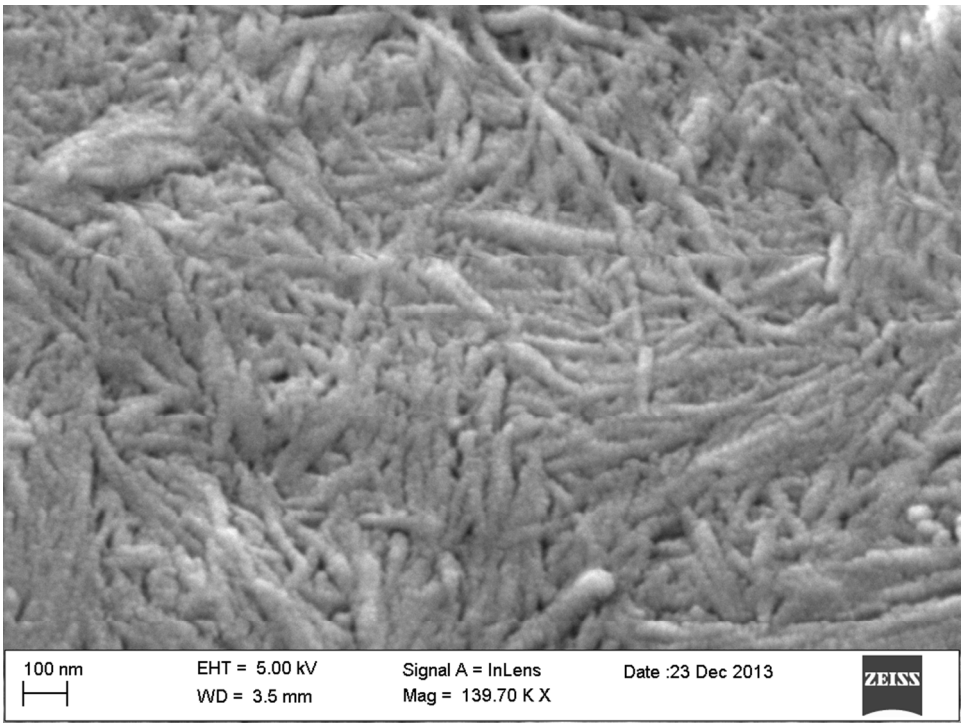

Figure 4a: FESEM image of C

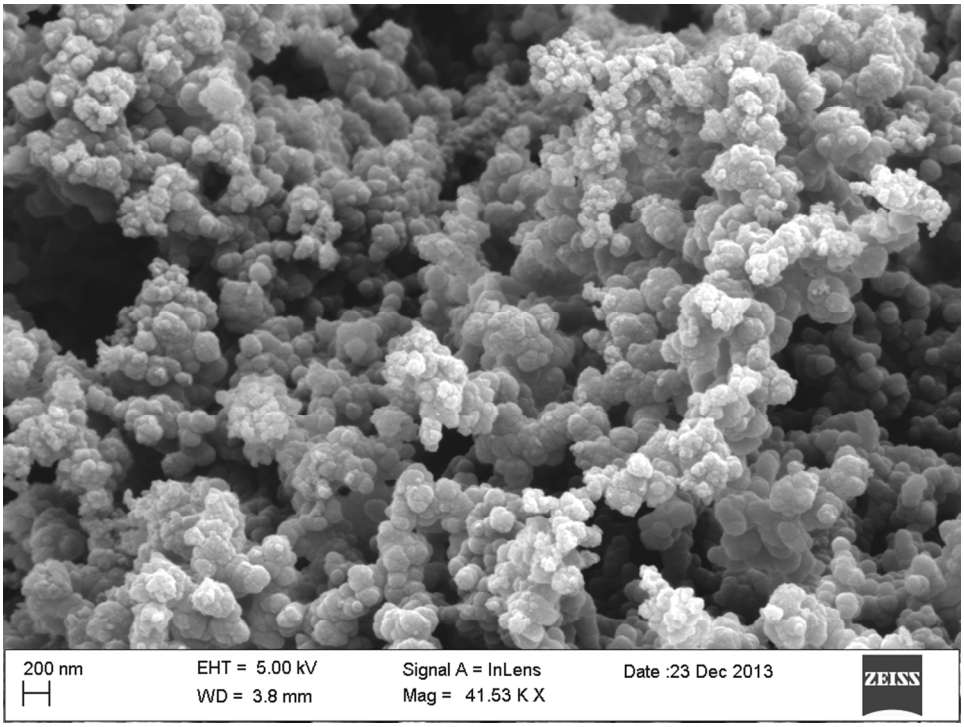

Figure 4b: FESEM image of PPy

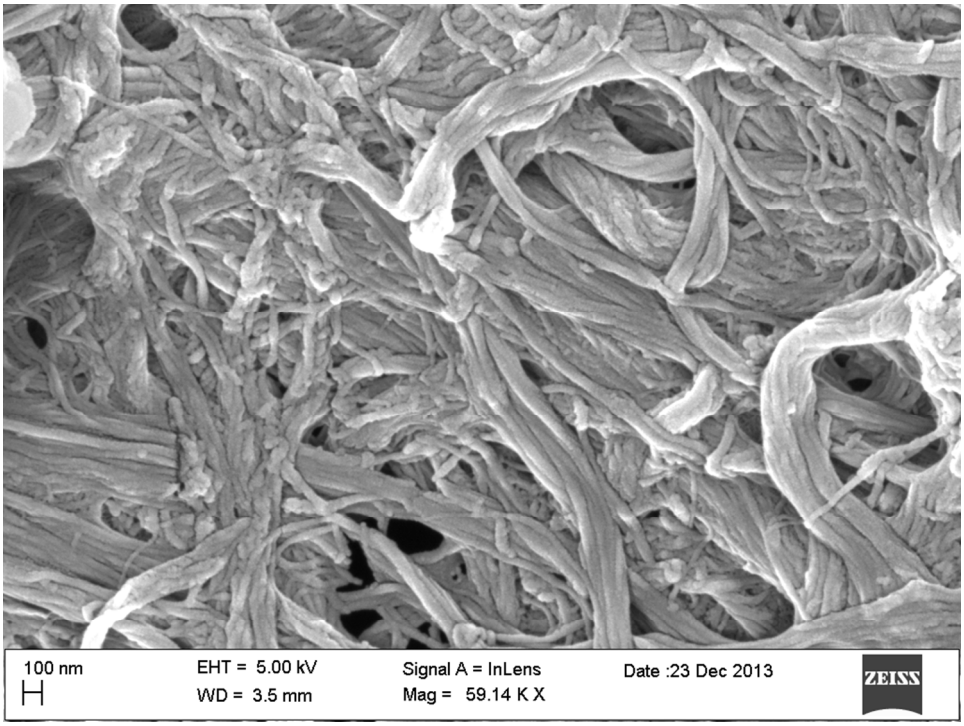

Figure 4c: FESEM image of CP

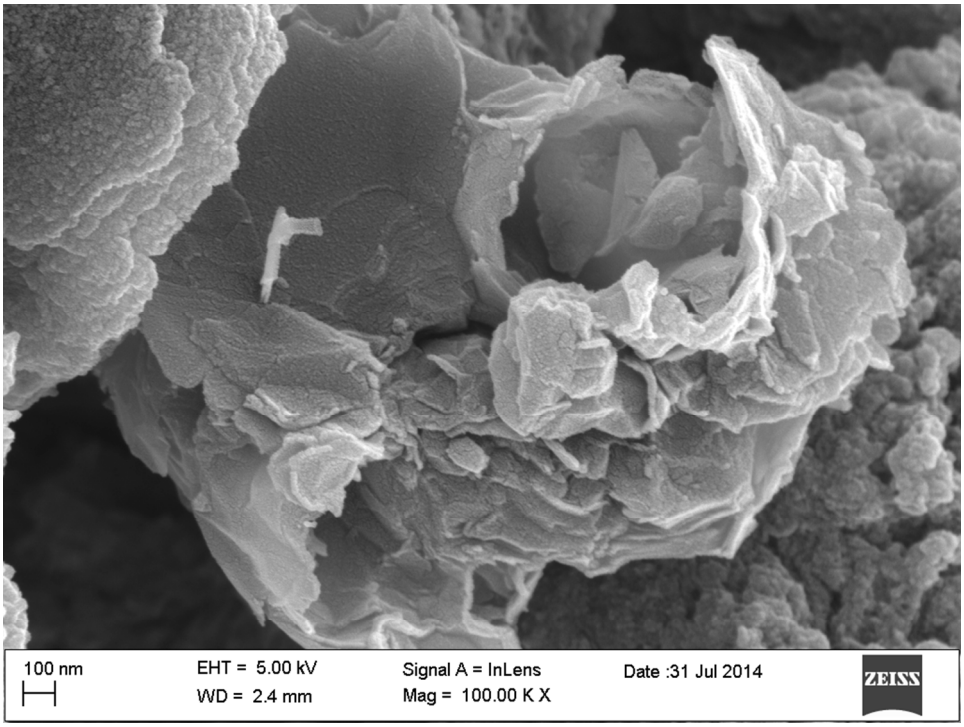

Figure 4d: FESEM image of GP

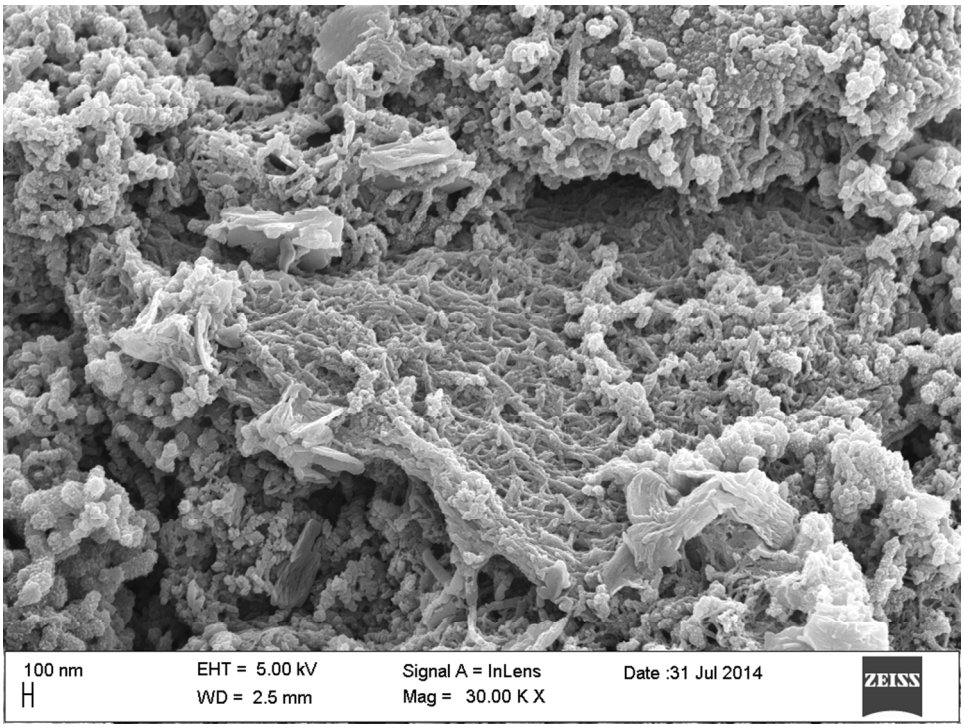

Figure 4e: FESEM image of CGP

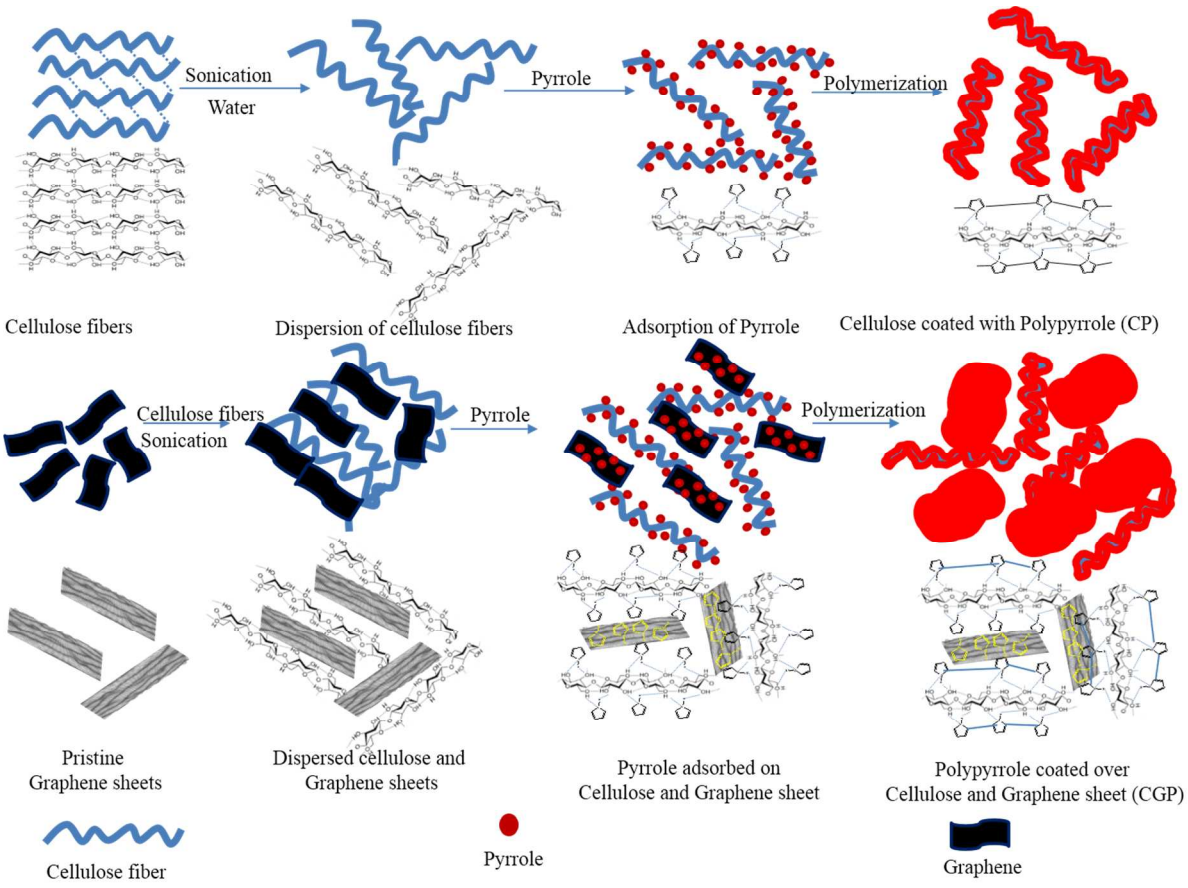

Figure 5: Schematic representation of Electrode formation

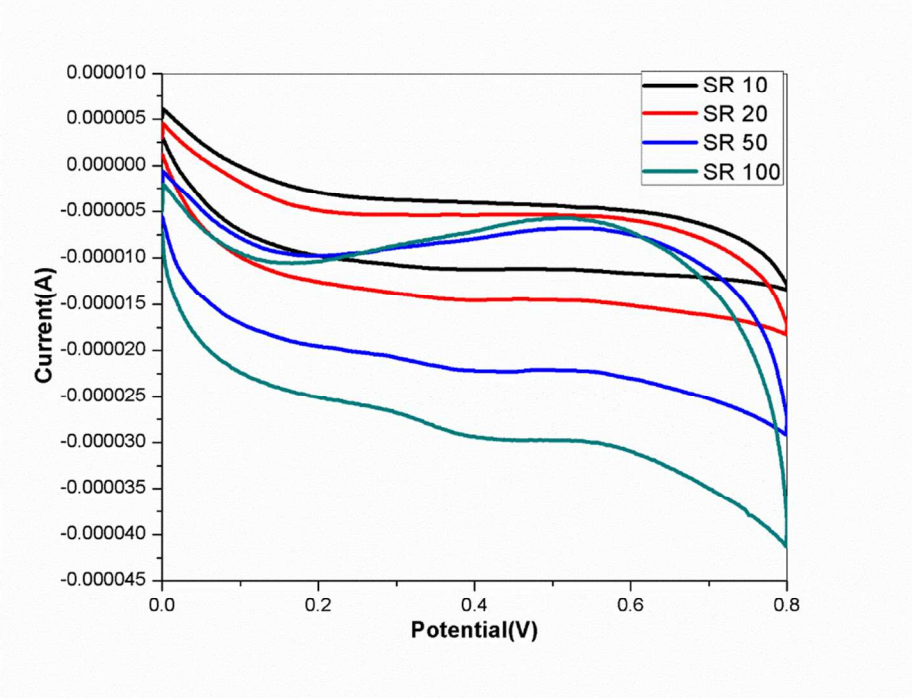

Figure 6a: CV Plots of C

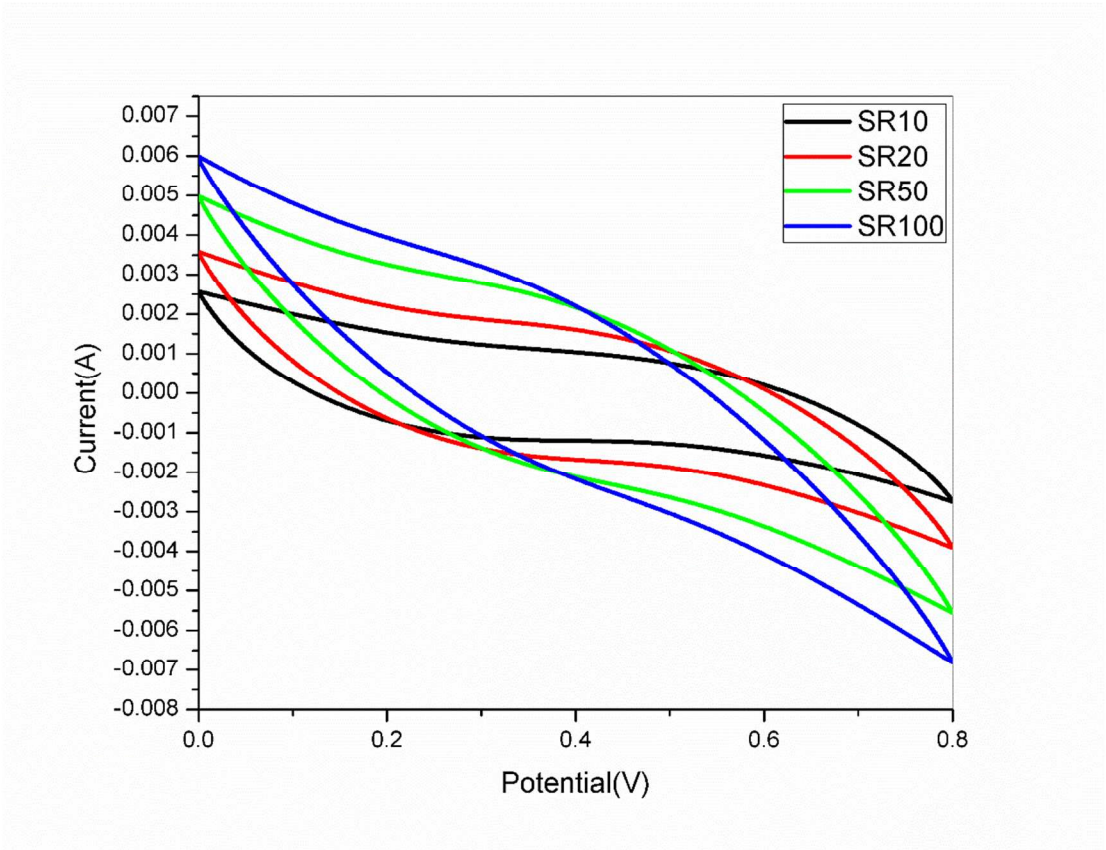

Figure 6b: CV Plots of PPy

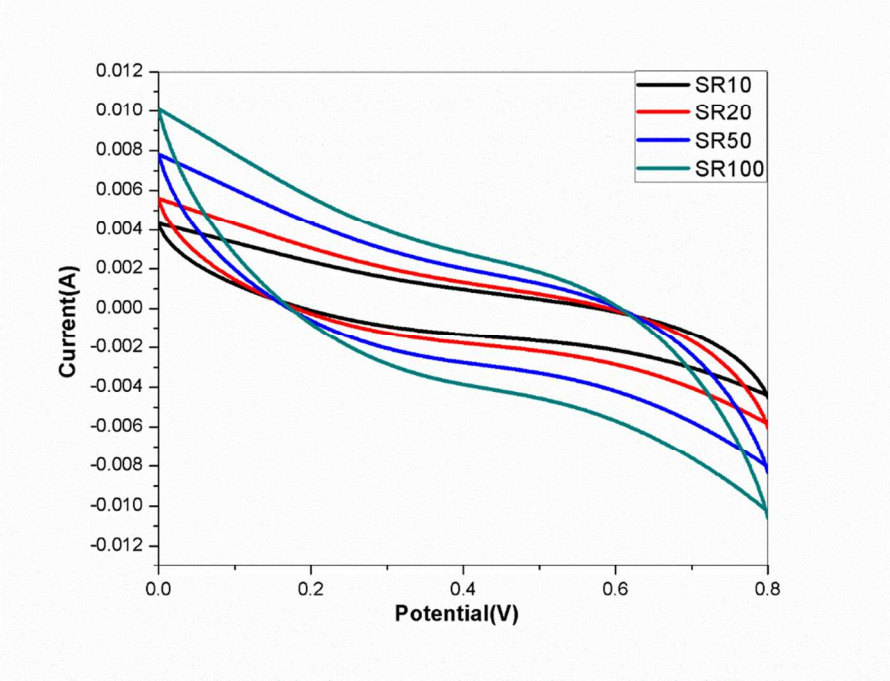

Figure 6c: CV Plots of CP

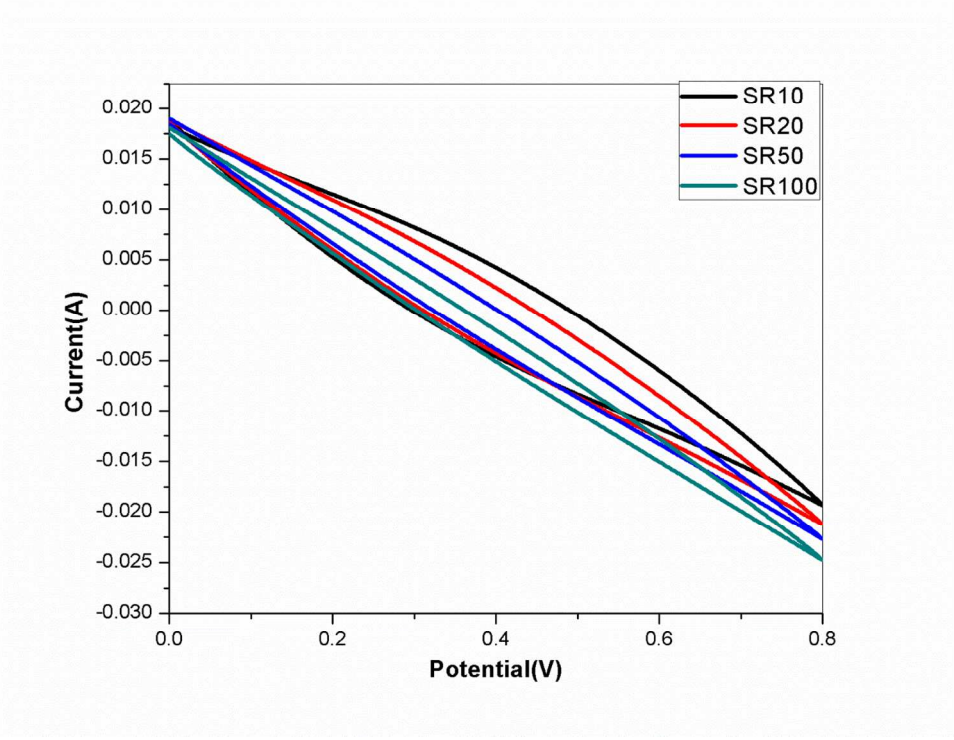

Figure 6d: CV Plots of GP

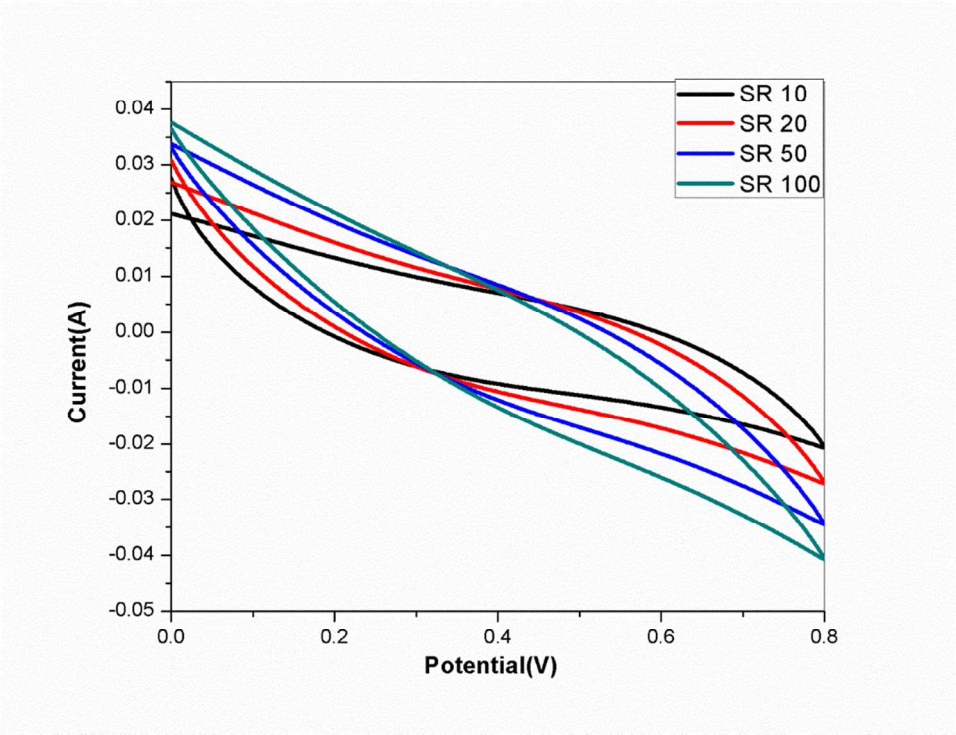

Figure 6e: CV Plots of CGP

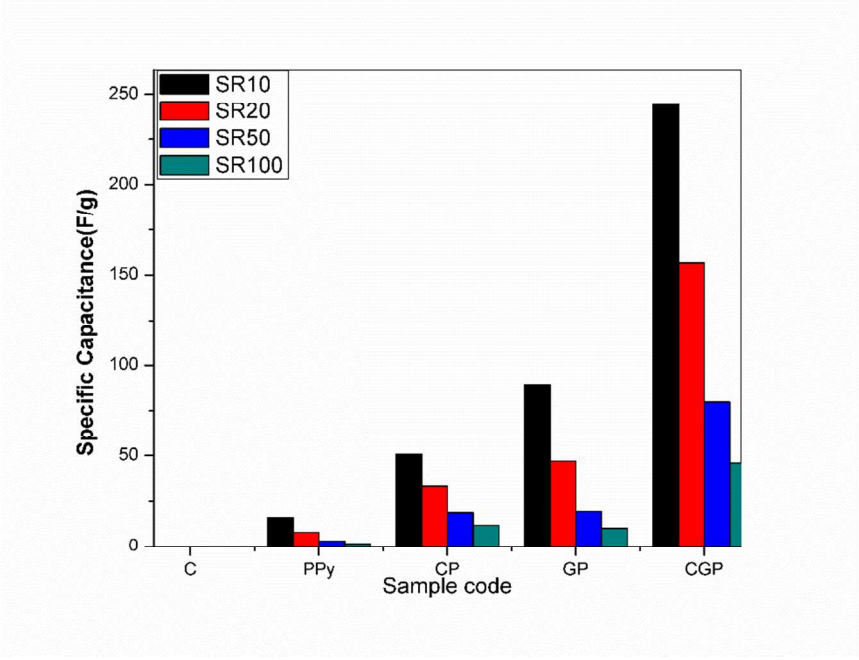

Figure 7a: Specific Capacitances of Electrode Materials

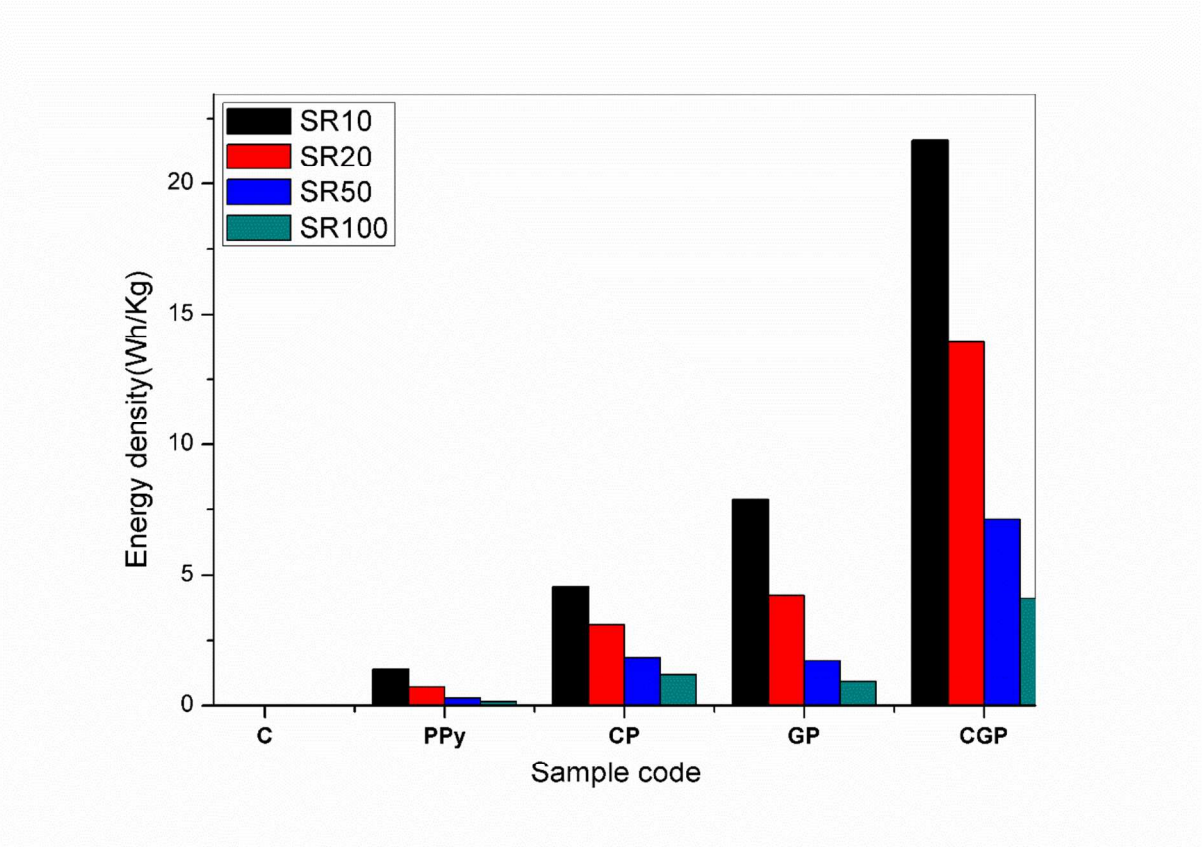

Figure 7b: Energy Densities of Electrode Materials

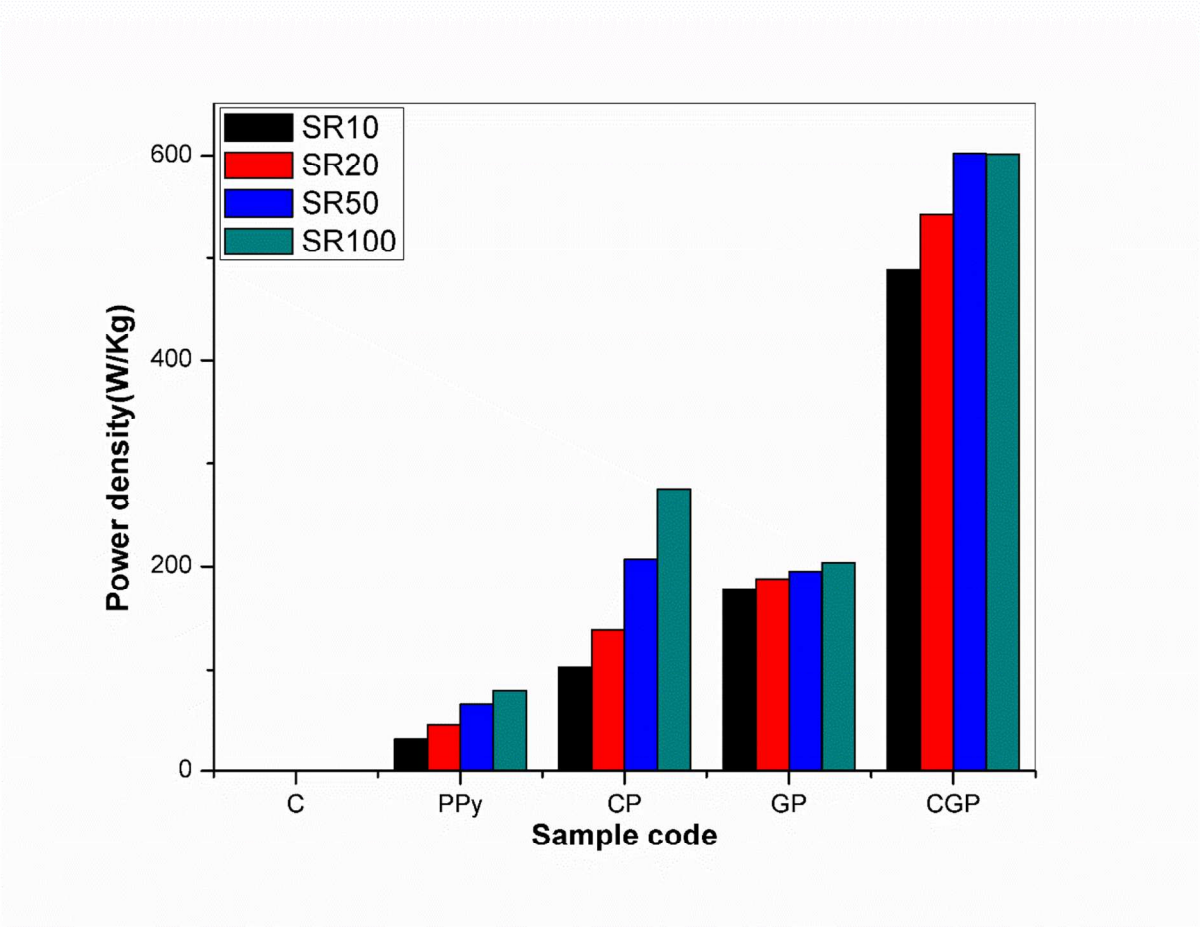

Figure 7c: Power Densities of Electrode Materials

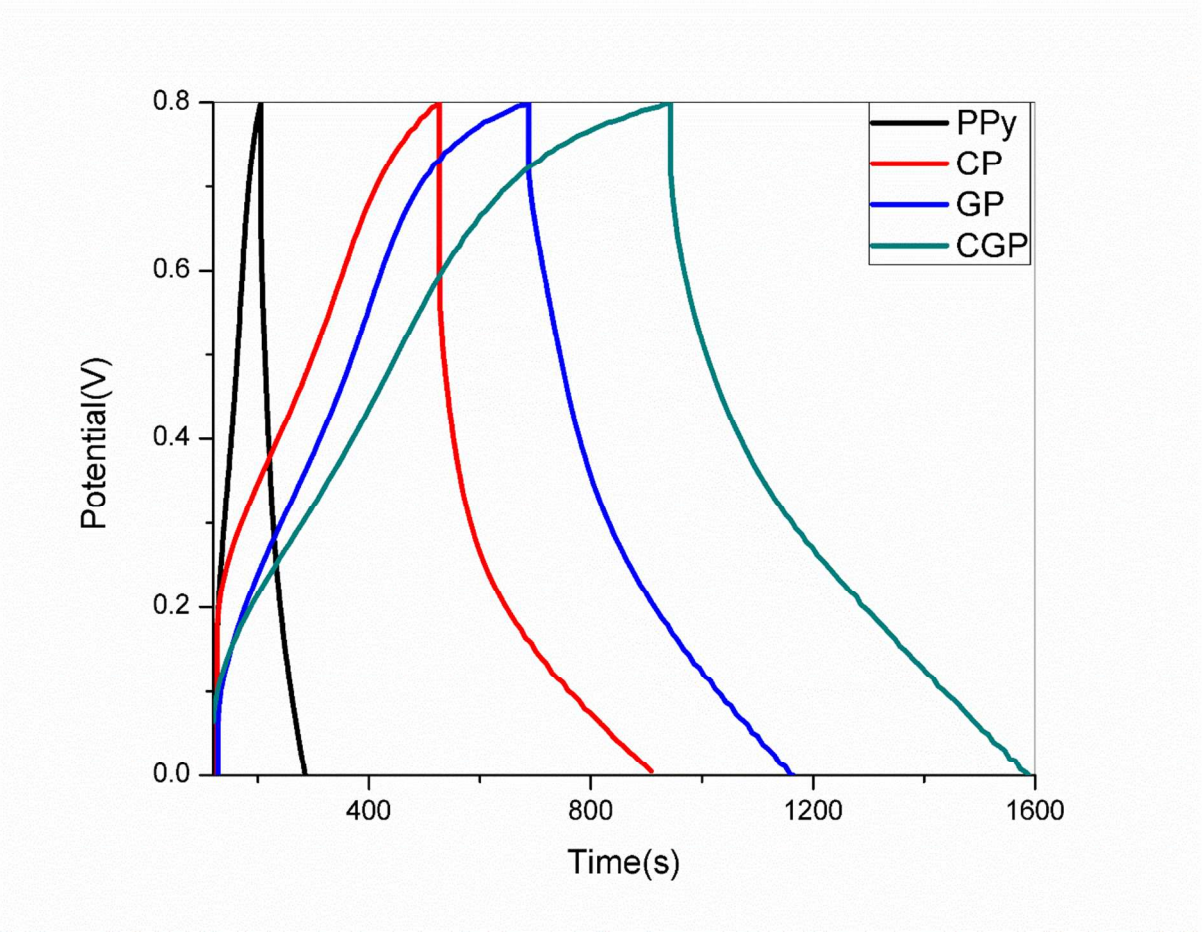

Figure 8: Galvanostatic Charge Discharge Nature of Electrodes

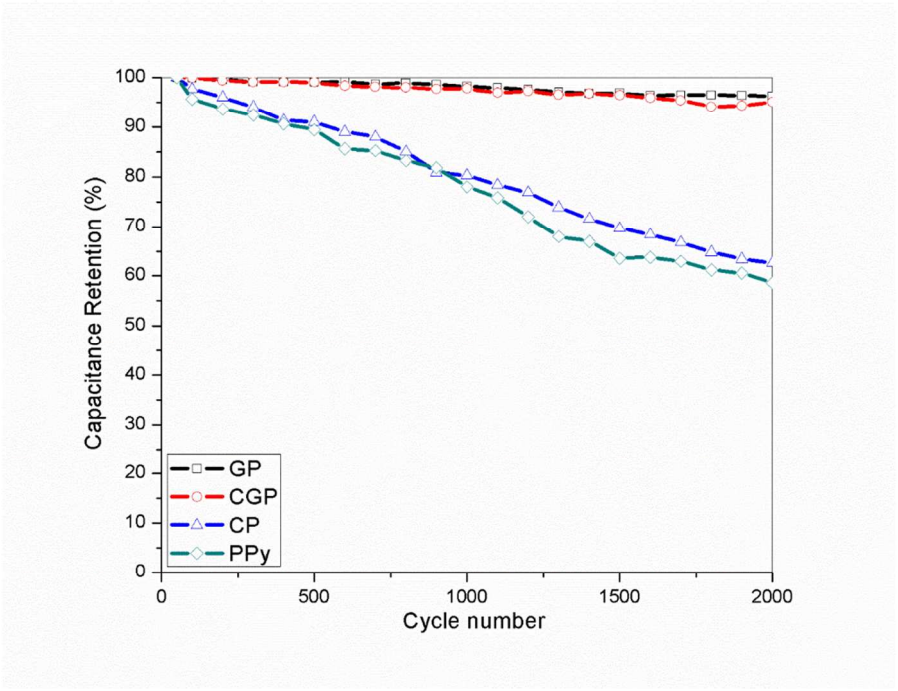

Figure 9: Cyclic Stabilities of Electrode Materials

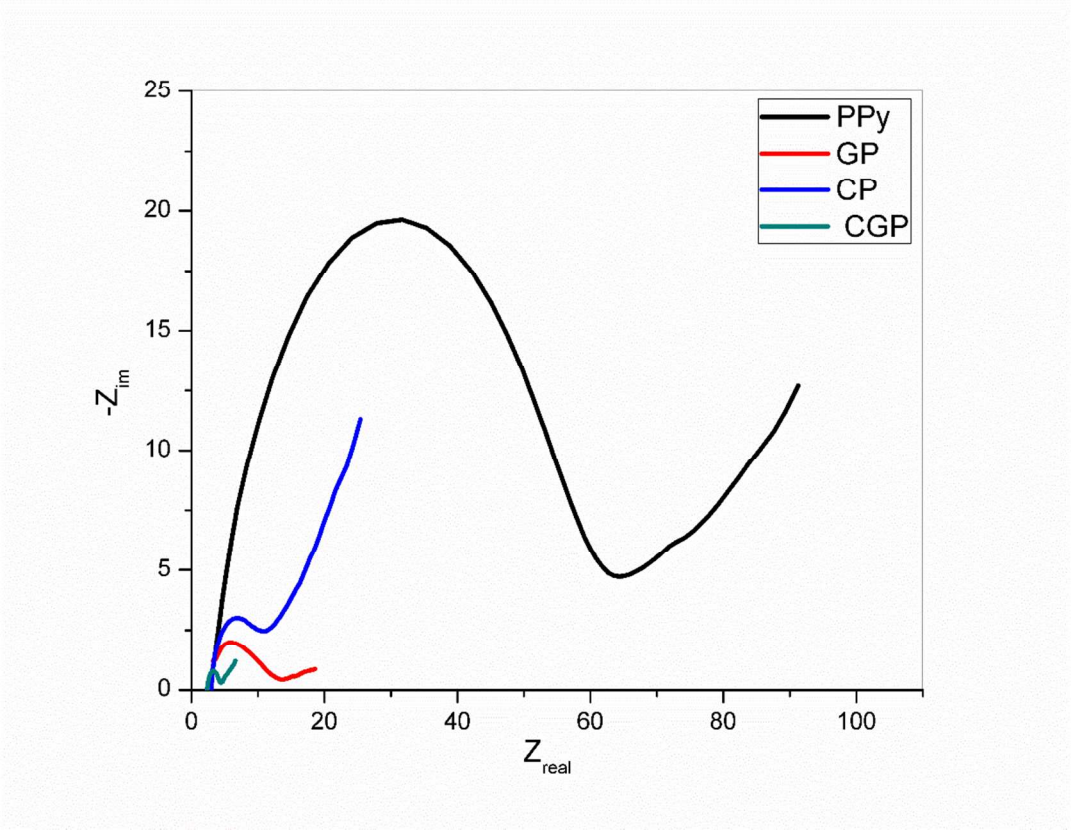

Figure 10: Impedance plots of Electrodes